Available online at www.sciencedirect.com
SCIENCE DIRECT®
ELSEVIER
Journal of Non-Crystalline Solids 326&327 (2003) 257–262
JOURNAL OF NON-CRYSTALLINE SOLIDS
www.elsevier.com/locate/jnoncrysol

Study of light-induced vector changes in the local atomic structure of As–Se glasses by EXAFS

G. Chen [a], H. Jain [a,*], Mir. Vlček [b], J. Li [c], D.A. Drabold [c], S. Khalid [d], S.R. Elliott [e]

[a] *Whitaker Laboratory, Department of Materials Science and Engineering, Lehigh University, 5 E. Packer Avenue, Bethlehem, PA 18015, USA*
[b] *Department of General and Inorganic Chemistry, University of Pardubice, 53210 Pardubice, Czech Republic*
[c] *Department of Physics and Astronomy, Ohio University, Athens, OH 45701, USA*
[d] *National Synchrotron Light Source, Brookhaven National Laboratory, Upton, NY 11973, USA*
[e] *Department of Chemistry, University of Cambridge, Cambridge CB2 1EW, UK*

Abstract

We have observed light-induced vector changes in the local structure of As–Se glasses using extended X-ray absorption fine structure (EXAFS) experiments with in situ laser illumination. Local structure around As and Se atoms was determined for as-prepared as well as annealed a-$As_{40}Se_{60}$ films, which were exposed to bandgap light of polarization parallel and perpendicular to that of the X-rays. For the as-prepared film, the nearest neighbor bond distance around Se atoms increases, the magnitude of which varies with the polarization of light, thus confirming our previous observations on a-$As_{50}Se_{50}$ films. These results give an atomistic indication of a light-induced vector expansion in any material, and provide insight of the mechanisms of the light-induced atom displacements.

1. Introduction

Many properties of semiconducting glasses based on chalcogens are known to be sensitive to the bandgap light [1–3]. The photons may affect the volume, amorphization, devitrification, mechanical, rheological, optical, electrical, or the chemical properties of the glass. In general, such changes in properties by light can be divided into vector and scalar effects, depending on whether or not the particular effect varies with the direction of the light polarization. Often the vector effects are a subset of the scalar effects, and much smaller in magnitude than the latter [4]. Among the vector effects, the light field-induced mass transport [5], photo-crystallization [6], and opto-mechanical effect [7] are particularly intriguing, which imply a change in the atomic structure that depends also on the polarization of light. For a long time, the light-polarization dependent phenomena were believed to occur exclusively in chalcogenide glasses. However, the observation of laser-induced birefringence in silica by Borrelli et al. [8] suggests that such phenomena are likely to be widespread and may extend to oxide glasses as well. These authors

* Corresponding author. Tel.: +1-610 758 4217; fax: +1-610 758 4244.
E-mail address: h.jain@lehigh.edu (H. Jain).

0022-3093/$ - see front matter © 2003 Elsevier B.V. All rights reserved.
doi:10.1016/S0022-3093(03)00403-4

suggest that the birefringence arises from an anisotropic volume change effected by the linearly polarized light exposure. Even though there are so many light-polarization dependent property-changes, the atomic-scale mechanism underlying these phenomena remains unclear. This lack of knowledge has been partly due to the fact that only a small fraction of sites participates in light-induced changes, and it is very difficult, if not impossible, to unravel the atomistics from measurements of such properties.

We have been investigating the atomistic origin of these so-called vector effects (which depend on the direction of the electric field vector of light, $\mathbf{E}_L$) by extended X-ray absorption fine structure (EXAFS) analysis around Se as well as As atoms in As_xSe_{1-x} films. The initial experiments were conducted on a-$As_{50}Se_{50}$ films [9]; the present paper reports new results on stoichiometric and As rich compositions ($x = 0.4$ and 0.57) in the as-prepared as well as annealed states. For observing a vector (or anisotropic) property the probe should also be anisotropic. The plane-polarized synchrotron radiation (for which the electric field ($\mathbf{E}_X$) of the X-rays is parallel to the ground plane) has allowed the identification of the direction of changes in local structure. Since the photo-induced changes can be temporary and/or permanent, we determined the structure under in situ conditions such that the laser and the X-ray beams overlapped on the sample.

2. Experiment

The amorphous chalcogenide As_xSe_{1-x} ($x = 0.4$, 0.5, 0.57) films were prepared by thermal evaporation of appropriate bulk glass pieces produced by the melt-quench method [10]. The evaporated films of 2 or 20 μm thickness were deposited on silica substrates (microscopy slides) in a vacuum of 10^{-5}–10^{-6} Torr at the rate of 1–2 nm/s. To avoid thickness and/or compositional inhomogeneity of films during deposition, the substrates were rotated in the evaporation chamber during evaporation. Some of the films were sealed in vacuum and annealed at ~10 °C below the respective glass transition temperature (T_g) for 1 h. The experiments were performed at beamline X-18b of the National Synchrotron Light Source, Brookhaven National Laboratory, using the experimental setup described previously [9]. The sample was irradiated with a He–Ne laser ($\lambda = 632.8$ nm, energy = 1.96 eV) light of approximately the bandgap energy ($E_g^{optical} \sim 1.8$ eV for a-$As_{40}Se_{60}$ [11]). The effective intensity of the beam on the sample is estimated to be 0.3 W/cm^2. The laser polarization is controlled by a zero-order half-wave plate (reflectivity < 0.5%) so that the direction of laser polarization is either horizontal ($\mathbf{E}_L$ nearly $\parallel \mathbf{E}_X$) or vertical polarization ($\mathbf{E}_L \perp \mathbf{E}_X$). The wavelength of the incoming X-rays is selected by a Si(1 1 1) channel-cut, double-crystal monochromator. Detuning and glitching shift devices with piezo-driven picomotors in the monochromator significantly improved the wavelength stability of the incident X-rays. Harmonic rejection was accomplished by detuning the monochromator to 70% of its maximum flux. The X-ray beam size was adjusted to 1×1 mm^2 to obtain good energy resolution at both the As and Se K-edges The laser beam intersected the X-ray beam at the sample, such that the former completely covered the area of the latter beam.

The samples were kept in dark before performing in situ laser illumination. For each composition, two sets of experiments were conducted in different regions of the same film. Within the first set, at least four continuous EXAFS scans were obtained at both As and Se K-edges to estimate the experimental uncertainty. Then the laser was turned on in a given polarization for 5 min and complete spectra were recorded during illumination. Next, the laser was turned off for 5 min before recording the next set of absorption data in the absence of light. The absorption edges around particular atoms were calibrated by using a neighboring region of the same sample as a reference. For the second set, the same procedure was repeated with the polarization of laser light rotated by 90°.

3. Results

Since As and Se K-edges are next to each other on the energy scale, their EXAFS spectra could be

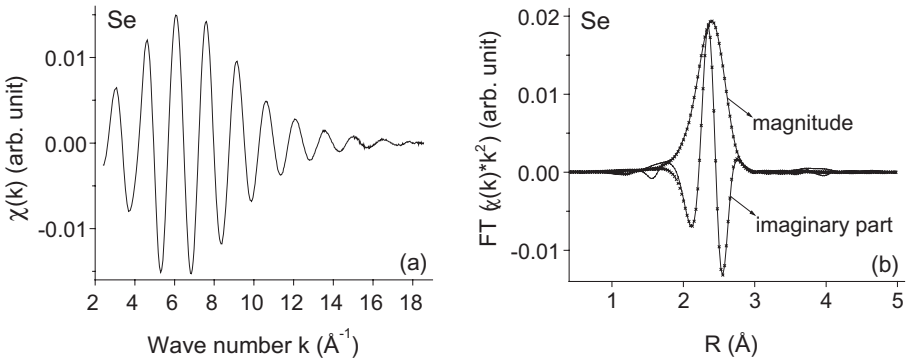

Fig. 1. (a) Typical EXAFS oscillation of a-$As_{40}Se_{60}$ film at Se K-edge. (b) Fourier transform of (a) gives the PRDF around Se atoms. The solid curves are experimental data and the '×' curves (mostly hidden under the solid curves) are the fittings to data.

obtained within the same scan. As an example, Fig. 1(a) shows the EXAFS oscillation for Se K-edge of an amorphous a-$As_{40}Se_{60}$ film. After Fourier transformation, the oscillation is transformed from k space to the real space. Fig. 1(b) shows the magnitude and imaginary part (solid curves) of the partial radial distribution function (PRDF) around Se atoms. The '×' symbol curves, mostly hidden under solid curves, are fitting to the data using standard data analysis programs with single scattering approximation [12]. Here we assumed the phase shift of scattered wave to remain unaffected by the small changes in the local environment. This is a minor assumption since As and Se are next to each other in the periodic table, and we are primarily interested in the relative changes induced by light. Usually four parameters are allowed to vary during data analysis: coordination number (CN), mean square relative displacement (MSRD), bond distance (R), and the absorption edge energy shift (ΔE_0). We find that CN has high correlation with MSRD, but low correlation with R and ΔE_0; R has high correlation with ΔE_0, but low correlation with CN and MSRD. Since the correlation between CN and MSRD will increase the uncertainty, we fixed the CN of Se as a constant of 2.1 during data analysis. By using the as-prepared film as a reference sample, we determined the absorption edge shift around a certain element with very high precision (e.g. for As K-edge ±0.02 eV and for Se K-edge ±0.05 eV). Within the experimental uncertainty, we did not find any absorption edge shift during the three sample stages for both elements. Since absorption edge shift (ΔE_0) and the average bond distance (R) are strongly correlated while doing the data analysis, we fixed ΔE_0 as a constant, and only let R vary during the parameter fitting. Thus, only two parameters are allowed to vary viz. the disorder parameter (MSRD) and the average bond distance (R).

The results of data analysis for a-$As_{40}Se_{60}$ film are shown in Fig. 2, where the sample stage AP means as-prepared film, ON means laser is turned on, and OFF means laser is turned off. Fig. 2(a) shows the results of nearest neighbor (NN) bond distance for Se atoms under different polarized light illumination. Here HP means $\mathbf{E}_L$ is parallel to the ground (the polarization plane of the X-rays), and VP means $\mathbf{E}_L \perp$ the ground. Fig. 2(b) shows the change in local disorder (MSRD) around Se atoms. The error bars for these parameters represent the actually observed range of maximum scattering within six consecutive scans during the AP stage. Similar results were obtained on one layer of 20 μm film, or 10 layers of 2 μm films. The unusually high accuracy of the data is due to the very high signal to noise ratio within the transmission mode and the fact that there was no physical change (in sample configuration) within a given set of experiment except for the change of polarization of light beam. From Fig. 2(a) we can clearly see that the NN bond distance increases during light illumination, and it remains the same after the laser is turned off. It is remarkable that

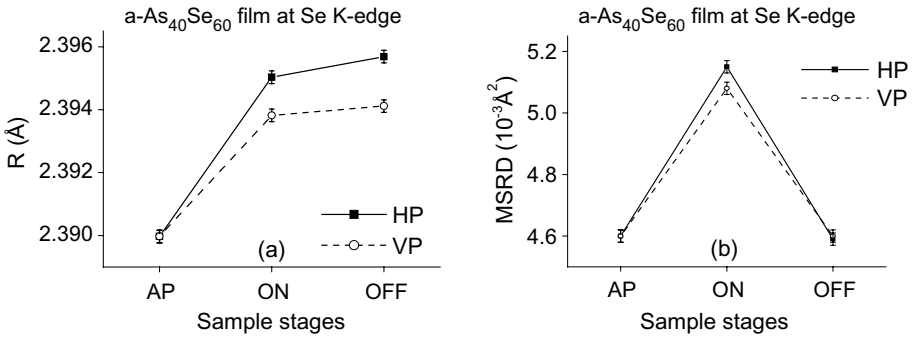

Fig. 2. (a) Se NN bond distance and (b) Se NN MSRD for different sample stages and different polarizations of the laser light. AP: as-prepared; ON: laser on; OFF: laser off; HP: horizontal polarization; VP: vertical polarization.

the increase in R also depends upon the polarization of the light: HP light creates greater expansion than the VP light does. The polarization dependent expansion around As atoms is not discernable within the experimental error (data not shown). From Fig. 2(b), we find that the light creates transient disorder around Se atoms, and it is almost completely recovered after the light is turned off. It is very interesting to see that during illumination (sample stage ON), the MSRD change around Se atoms is also polarization dependent, which means the transient structural disorder around Se is larger along the direction of the laser polarization than to the perpendicular direction.

Similar light-polarization dependent photo-expansion was also observed in a-$As_{50}Se_{50}$ film [9]. However, for a-$As_{57}Se_{43}$ film, the expansion for the NN bond distance around As and Se atoms is much smaller than in the a-$As_{40}Se_{60}$ and a-$As_{50}Se_{50}$ samples. Therefore, it is difficult to observe the polarization-dependent effects in this material.

In general, the properties of as-prepared films are not exactly the same as of the annealed films, so it is interesting to compare the light-induced and heat-induced changes in the local structure. Fig. 3 describes light-induced structural changes around Se atoms in the annealed a-$As_{40}Se_{60}$ films. It shows the NN bond distance and the local disorder for the as-annealed (AN), as well as the ON and OFF stages. Instead of the increase shown by the as-prepared (unannealed) films (Fig. 2(a)), for this case the NN bond distance decreases slightly during illumination, and is partly recovered on turning off the laser. For the MSRD, the light creates similar effects in the annealed film as in the as-prepared film.

We wish to emphasize the error bars as shown in Figs. 2 and 3. Typically, there are two kinds of

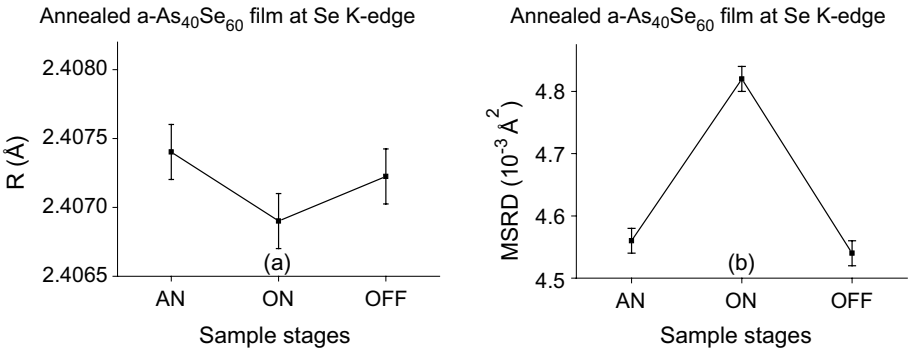

Fig. 3. (a) Se NN bond distance and (b) Se NN MSRD for different sample stages.

error bars: one is from the difference between the true value and the measured value, or the so-called accuracy; the other is from the difference between the average measured value and the measured value, the so-called precision. In EXAFS, the accuracy is determined by many factors including theoretical modeling, sample conditions, etc.; the error bar from such sources is relatively large (e.g. for bond distance, it is typically from ±0.005 to ±0.01 Å). Since we are interested in the relative changes during the in situ experiment, precision is of primary interest to us. It is much smaller in our experiments than the accuracy. When we use X-rays to probe the same region of the sample for several continuous scans, the precision in R is obtained as $\pm 2 \times 10^{-4}$ Å, with high reproducibility between several different sets of samples.

4. Discussion

4.1. Photo-induced scalar changes in the local structure

Before we discuss the vector changes in our glass films, it is necessary to understand the much stronger scalar changes first. We know that As and Se form a nearly covalent compound, with covalent radii of 1.21 Å for As and 1.17 Å for Se [13]. Therefore, it can be expected that the NN covalent bond distances increase in the order of Se–Se < As–Se < As–As. In thermally evaporated film, the high quench rate can affect the sample homogeneity with the possibility of As and Se rich regions existing within the otherwise homogeneous structure. Under light illumination, the photo-chemical reaction As–As + Se–Se → 2As–Se may occur in the film, similar to that observed in the a-$As_{40}S_{60}$ film by Raman spectroscopy [14]. These photo-chemical reactions can be the photo-polymerization of As_4Se_4 and/or As_4Se_3 molecules with excess Se, as proposed earlier by Frumar et al. [14,15]. The result of such photo-chemical reaction would be to increase the NN bond distance around Se and decrease the NN bond distance around As. In our experiment, an increase of NN bond distance around Se is observed (Fig. 2(a)), but the As NN bond distance increases instead of decreasing (data not shown), which implies a more complex light-induced change than this particular photo-chemical reaction.

By comparing the average NN bond distance in the as-prepared and annealed films (Figs. 2(a) and 3(a)), we find an increase in the NN bond distance as a result of annealing. This observation is in apparent disagreement with the observed densification on annealing [16], which would normally manifest in a concurrent decrease of R. We believe that the densification occurs primarily through the rearrangement of the intermediate range structure as proposed by Shimakawa et al. [17]. Note that the light has the same tendency of increasing the NN bond distance as annealing. Therefore, we propose, in addition, a local expansion of bonds around the two elements by some kind of relief of strains, which were introduced during rapid quenching.

For annealed films, the NN bond distance around Se atoms decreases during illumination (Fig. 3(a)), possibly due to bond breaking and the formation of light-induced defects.

4.2. Photo-induced vector change in the local structure

Based on the mechanism of scalar changes discussed above, we propose the following explanation for the photo-induced vector change in the NN bond distance around Se atoms: the absorption of approximately bandgap light promotes electrons to low-lying unoccupied conduction-band (antibonding) states, which can cause bond breaking. The electron–hole pair recombination process can lead to the photo-chemical reaction as discussed above. For the Se atoms, the lone pairs are excited and aligned by the light along its polarization direction [18]. When the excited lone pairs see other excited As atoms, they have an enhanced probability to form an As–Se bond with such atoms along that direction. For example, when we use HP light to illuminate the sample, there are new As–Se bonds forming parallel to the ground at the expense of the existing Se–Se bonds. In analyzing our data we have fixed the coordination number of Se, in accordance with the results of the molecular dynamic simulations [19,20].

Since synchrotron X-rays are polarized parallel to the ground, the ejected photo-electrons detect the neighbors aligned preferentially parallel to the ground plane. (The photo-electrons have a distribution weighted according to $\cos^2\theta$, where θ is the angle between the X-ray polarization direction and the direction of the ejected photo-electrons [21].) It means that the HP light should produce a larger increase in bond distance than the VP light, as observed in our experiment. The reason why excited lone pairs of Se atoms should be aligned along the polarization of the light is not clear, but we suspect that the high electronic polarizability of Se atoms should make such alignment easier. In any case, the anisotropic formation of bonds under the illumination of differently polarized light provides an atomistic view of photo-induced anisotropic mass transport or photo-crystallization.

5. Summary

In conclusion, we have directly observed a light-polarization dependent elongation of the nearest neighbor bond distance around Se atoms in a-$As_{40}Se_{60}$ film. This local expansion effect is very similar to what we have found earlier in a-$As_{50}Se_{50}$ films. Anisotropic local expansion around Se atoms occurs as bandgap light reorients Se LP's, and helps form anisotropic As–Se bonds. Such polarization dependent change in structure is not discernable for as-prepared a-$As_{57}Se_{43}$ and annealed a-$As_{40}Se_{60}$ films that have more stable local disorder than the as-prepared $As_{40}Se_{60}$ and $As_{50}Se_{50}$ films. Our experiments provide an atomistic view of photo-induced vector effects in chalcogenide glasses.

Acknowledgements

We thank the US National Science Foundation for supporting this work under Grants DMR 00-74624 and DMR 00-81006. MV thanks support from MSMT Czech Republic under Grant ME471.

References

[1] K. Shimakawa, A. Kolobov, S.R. Elliott, Adv. Phys. 44 (1995) 475.
[2] K. Tanaka, Semiconductors 32 (1998) 861.
[3] H.S. Nalwa, in: Chalcogenide Glasses and Sol–Gel Materials, Handbook of Advanced Electronic and Photonic Materials and Devices, vol. 5, Academic Press, 2001.
[4] I. Janossy, A. Jakli, J. Hajto, Solid State Commun. 51 (1984) 761.
[5] A. Saliminia, T.V. Galstian, A. Villeneuve, Phys. Rev. Lett. 85 (2000) 4112.
[6] V. Lyubin, M. Klebanov, M. Mitkova, T. Petkova, J. Non-Cryst. Solids 227–230 (1998) 739.
[7] P. Krecmer, A.M. Moulin, R.J. Stephenson, T. Rayment, M.E. Welland, S.R. Elliott, Science 277 (1997) 1799.
[8] N.F. Borrelli, C.M. Smith, J.J. Price, D.C. Allan, Appl. Phys. Lett. 80 (2002) 219.
[9] (a) G. Chen, H. Jain, M. Vlcek, S. Khalid, D.A. Drabold, S.R. Elliott, Nat. Synchr. Light Source Sci. Highlights (2001) 2–22, Also see <http://www.pubs.bnl.gov/documents/23813.pdf>;
(b) G. Chen, H. Jain, M. Vlček, J. Li, D.A. Drabold, S.R. Elliott, Appl. Phys. Lett. 82 (2003) 706.
[10] H. Jain, S. Krishnaswami, A.C. Miller, P. Krecmer, S.R. Elliott, M. Vlcek, J. Non-Cryst. Solids 274 (2000) 115.
[11] J.P. De Neufville, S.C. Moss, S.R. Ovshinsky, J. Non-Cryst. Solids 13 (1973–1974) 191.
[12] WINXAS program: http://www.winxas.de; FEFF program: http://feff.phys.washington.edu.
[13] K.S. Liang, J. Non-Cryst. Solids 18 (1975) 207.
[14] M. Frumar, Z. Polak, Z. Cernosek, J. Non-Cryst. Solids 257 (1999) 105.
[15] M. Frumar, M. Vlcek, Z. Cernosek, Z. Polak, T. Wagner, J. Non-Cryst. Solids 213&214 (1997) 215.
[16] Y. Kuzukawa, A. Ganjoo, K. Shimakawa, Y. Ikeda, Philos. Mag. B 79 (1999) 249.
[17] K. Shimakawa, N. Yoshida, A. Ganjoo, Y. Kuzukawa, J. Singh, Philos. Mag. Lett. 77 (1998) 153.
[18] I. Janossy, J. Hajto, W.K. Choi, J. Non-Cryst. Solids 90 (1987) 529.
[19] J. Li, D.A. Drabold, Phys. Rev. Lett. 85 (2000) 2785.
[20] J. Li, D.A. Drabold, Phys. Rev. B 61 (2000) 11998.
[21] See, for example E.A. Stern, in: D.C. Koningsberger, R. Prins (Eds.), X-ray Absorption: Basic Principles of EXAFS, SEXAFS, and XANES, Wiley, New York, 1988.